Journal of Rehabilitation in Civil Engineering 8-4 (2020) 118-136

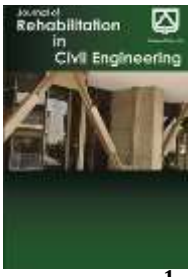

journal homepage: http://civiljournal.semnan.ac.ir/

Numerical and Physical Modeling of Soft Soil Slope Stabilized with Stone Columns

E. Naderi[1], A. Asakereh[2*], M. Dehghani[3]

1. Ph.D. candidate, Department of Civil Engineering, University of Hormozgan, Bandar Abbas, Iran
2. Assistant Professor, Department of Civil Engineering, University of Hormozgan, Bandar Abbas, Iran
3. Assistant Professor, Department of Civil Engineering, University of Hormozgan, Bandar Abbas, Iran

Corresponding author: *asakereh@hormozgan.ac.ir*

ARTICLE INFO

Article history:
Received: 01 January 2020
Accepted: 29 July 2020

Keywords:
Bearing capacity,
Stone column,
Strip footing,
Safety factor,
Slope.

ABSTRACT

There can be many reasons for engineers to place the footings near a slope such as leakage of suitable sites or architectural considerations. One of the approaches to increase the amount of bearing capacity, especially in soft soils, is adding stone columns to the soil. In this research, the behavior of a strip footing placed near a stone column reinforced clayey slope was investigated. For this purpose, some small-scale model tests were performed on a clayey slope reinforced with stone columns. The effects of the length of the stone column and the length of encasement on the footing were studied. Additionally, vertical encased stone columns in a group arrangement were investigated. Some numerical analyses were also performed using the Midas GTS NX finite element software, and the factor of safety was studied. Results show that the optimum length was equal to four times the diameter of stone columns. It was observed that by increasing the length of encasement, the bearing capacity of strip footing was also increased. The safety factor of slope showed an increase when stone columns were added to the slope, but the maximum influence on the factor of safety appeared when the stone column was in the upper middle of the slope.

1. Introduction

Soft soils usually make some problems for structures, such as excessive settlement, deformation, and stability problems. One of the geotechnical solutions for soft soils is adding column-like elements called stone columns to the soil. The behavior of the ordinary stone columns added to clay soil is studied by many researchers using experimental model tests [1-4]. They all reported a decrease in settlement and an improvement in the bearing capacity of stone column reinforced soils. The efficiency of

DOI: 10.22075/JRCE.2020.19431.1367

stone columns is related to the confining pressure of the surrounding soil The lateral confinement may not be enough for very soft soils, and bulging failure can occur at the upper parts of the stone column which causes a reduction in the effectiveness of stone columns [5]. Thus, providing additional confinement by vertical encasing of stone columns with geosynthetics is necessary for such soils. Experimental studies on vertical encasing of the stone columns with geosynthetics have been carried out widely [6-11]. Vertical encased stone columns have been numerically investigated by some researchers [10, 12-16]. All experimental and numerical investigations showed that the behavior of the stone column was improved by using vertical encasement.

There are many conditions that a footing must be built adjacent to a slope. Construction of a footing adjacent to a slope affects the behavior of footing. It makes the bearing capacity reduced compared to the bearing capacity on the flat ground [17]. Generally, the slope should get modified with appropriate stabilization techniques to improve the bearing capacity of footing and to protect the slope from failure. Many researchers have investigated the improvement of slopes using soil reinforcement techniques in the horizontal form [18-21]. Stabilizing the slope with the vertical form of reinforcement has been studied by other researchers [22-24].

Improving the soft soil underneath the embankments with stone columns was studied by some researchers [25-27]. Reinforcing a slope with stone columns can also be another way for improving the slope stability and bearing capacity of the adjacent footing. Ghazavi and Shahmandi have presented a numerical analysis using GEO-OFFICE software along with a closed-form solution on limit equilibrium method to study the stability of stone column reinforced slopes [28]. Results show that the best location of the stone column is around the crown of the slope. Vekli et al. investigated the treatment of the strip footing adjacent to clayey slopes reinforced with stone columns using model tests and the PLAXIS software [29]. Both numerical and experimental results show that the bearing capacity of the strip footing increases with reinforcing the slope with a stone column. Hajiazizi et al. investigated the stabilization of a sand slope with the stone column and determined the optimal location for the column [30]. An experimental study was conducted for a saturated two-layer sand slope and the results were verified with a 3D numerical analysis. Raee et al. numerically and experimentally studied the effect of stone column on the behavior of a strip footing placed on a sand slope and investigated some parameters such as rigidity of the stone columns and the spacing between them [31]. The findings of this study showed that increasing the rigidity and decreasing the spacing between the stone columns increases the bearing capacity of strip footing. Naderi et al. studied the improvement effects of the stone column on the behavior of a strip footing placed on a clayey slope [32]. The location of ordinary and vertical encased stone columns and also the efficiency of the group of ordinary stone columns were investigated in this study. Nasiri and Hajiazizi used a series of laboratory model tests and a 3D finite difference model to investigate the behavior of geotextile encased stone columns in the stabilizing of sandy slopes [33]. Results showed that the use of encased stone columns for stabilizing the slopes is an

efficient way to increase the bearing capacity and the safety factor.

Despite the aforementioned researches, insufficient study is done on the behavior of the strip footing placed on a stone column reinforced slope. Also, the effects of the stone column length, length of the encasement, and the group of vertical encased stone columns on the behavior of the slope are not investigated. Hence, this paper presents a study on the effect of these parameters on the behavior of a strip footing adjacent to a soft clay slope. Both types of ordinary stone columns (OSCs) and vertical encased stone columns (VESCs) were tested in different situations. Then, a finite element modeling with Midas GTS NX software was carried out, and the stress distribution and safety factor were investigated. Moreover, the effects of some parameters such as the location of the column and the effect of a group of OSCs on the safety factors were determined using numerical analyses.

2. Physical Modeling

2.1. Properties of Materials

In order to determine the properties of materials, some preliminary standard tests were performed. Material properties are listed in Table 1. The stone column material was selected with aggregate size with a range of 2-10mm, considering the scale effect and the size of the model footing.

In very soft soils (with cu<15kPa), the confinement provided by the surrounding soil is not sufficient and the stone column cannot perform well in carrying the required bearing capacity [5,6,8]. Thus, some undrained shear strength tests (according to ASTM D2166-06 [34]) were performed on clay soil with different water contents. The results of the tests determined that the amount of the water content of clay with cu=15kPa was equal to 25%. Therefore, we used the clay with this water content in all the tests.

Table 1 Material properties.

Clay		Stone column		Encasement	
Parameter	Value	Parameter	Value	Parameter	Value
Liquid limit (%)	31	Specific gravity	2.7	Material	polyethylene
Plastic limit (%)	17	Unit weight at 66% relative density (kN/m^3)	16	Ultimate tensile strength (kN/m)	8
Plastic index (%)	14	Internal friction angle (Ø) at 66% relative density	45	Strain at ultimate strength (%)	48
Unit weight at 25% water content (kN/m^3)	20	Uniformity coefficient (C_u)	1.44	Secant stiffness at ultimate strain (J) (kN/m)	16.67
Undrained shear strength (kPa)	15	Curvature coefficient (C_c)	0.93	Openings size (mm)	2×2
Unified system classification	CL	Unified system classification	GP	Mass (g/m^2)	190

2.2. Experimental Setup

The apparatus designed for this research is consisting of two main parts including a test tank and a loading system. The loading system includes a hydraulic power unit connected to a hydraulic piston with two high-pressure hoses. The capacity of the hydraulic jack was 4 tons. A pressure gauge was installed on the hydraulic unit which was calibrated with a load cell before the tests. The gauge was used to determine the applied load on the footing.

In the experiments, a longitudinal slice of an assumed stone column reinforced slope was studied. This slide can be expanded from both sides in practice. Dash and Bora showed that the optimum spacing between centers of the stone columns in group pattern is three times of their diameter [35]. Therefore, the width of the longitudinal slice was considered equal to 30cm. The test tank dimensions are selected to make the stress in the soil applied from the loading would be almost zero at the bottom, right and left boundaries of the tank for all states of the test. All inner surfaces of the tank were coated with grease to decrease the friction between the clay and boundaries. In fact, the stress that reaches the front and back sides of the tank represents the stress which transfers from beside imaginary rows in the group pattern of stone columns. It should be noted that for this purpose, the length of the strip footing should be 30cm instead of 29cm. This 1cm gap was considered to make it possible in all the tests to put and pick up the footing. Thus, a tank was built to accommodate the clay slope with the schematic design shown in Fig. 1. The location of the footing was constant in all the tests and the distance between the center of the footing to the slope crown was 10cm. The slope angle was 45˚ and was constant in all the tests. In this figure, Δ represents the horizontal distance between the center of the footing to the center of the stone columns. The test tank was made of steel and some steel straps were welded around it to prevent the deformation at high loading levels. One side of the soil tank has two tempered glasses to easily check the slope during the construction and observation of the deformations during the loading. The loading support was a rigid frame that was welded all around the tank. The top side of the frame was a 30cm width IPE16 beam with a plate for locating the hydraulic piston. The test apparatus which was constructed for the current study can be seen in Fig. 2.

The model strip footing dimensions were 29cm length, 10cm width, and 4cm height and it was made of steel. Two dial gauges with a sensitivity of 0.01mm were used to measure the vertical displacement of footing. The average of the measured settlements of gauges was assumed as displacement of the footing. These gauges were placed on both sides of the footing as shown in Fig. 3.

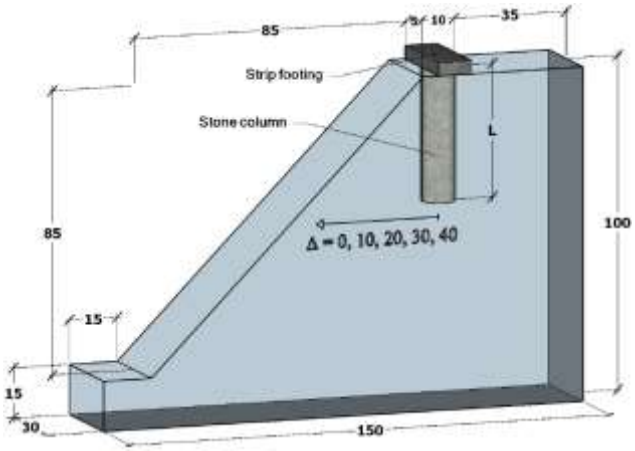

Fig. 1. Dimensions of the clay slope and location of footing and stone column (unit: cm).

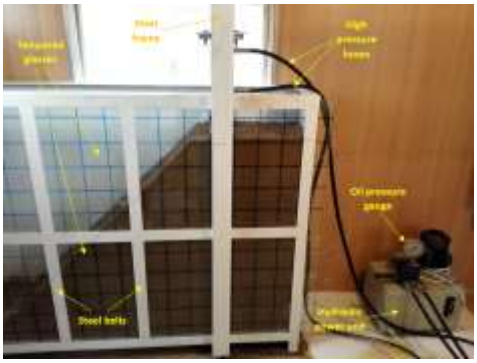

Fig. 2. Test apparatus and clay slope.

Fig. 3. Dial gauges in both sides of the footing.

2.3. Preparation of Soft Clay

A mineral clay from the Fars province in Iran was used in the laboratory tests. The initial natural moisture content of the clay was 4%. The soil was prepared at a moisture content of 25%, corresponding to 15kPa undrained shear strength. Therefore, some additional amount of water was weighed and added to the clay. They were mixed well to make the moisture uniform. Then, to guarantee the uniformity of water content within the clay, the moisturized soil was kept in plastic bags for seven days. The bottom of the tank was covered with nylon before filling to prevent losing the moisture.

To make access to the bottom part of the test tank easy, the upper glass was removed during the construction of the bottom half of the slope. The clay was filled in the test tank in 5cm thick layers. The volume of each 5cm layer of clay was calculated according to the level of the slope at that layer, and then the weight of the layer was determined using unit weight equal to 20kN/m^3. Next, the clay was weighted and placed at the assumed level. A tamper with 6.8kg mass and 25cm×25cm dimensions in plan was built and used for compacting the clay. The drop height of the tamper was 20cm and the soil surface was compacted till the 5cm layer was placed at the right level. The average of the number of blows was about 5 times. With this effort, a uniform compaction of clay with a certain bulk unit weight and a leveled surface was achieved. This 5cm compaction effort was repeated till the slope was completed. Some controlling random specimens were taken from compacted clay to ensure that the properties of clay were kept constant in all the tests and the results showed negligible variations.

2.4. Construction of Stone Columns

The replacement method was used for constructing all the stone columns in the small scale tests. The replacement method was already exerted by many other researchers [1, 6, 7, 29, 36]. A cylindrical pipe made of galvanized iron with a diameter of 10cm was used for the construction of the stone columns. All stone columns were constructed with a diameter of 10cm. Both sides of the pipe were lubricated with oil to decrease the friction between the soil and pipe. Therefore, the penetrating and withdrawing the pipe was done easily and the disturbance in the clay soil was minimum. Then the pipe was inserted into the soft clay, and the inside soil was excavated. We tried to be sure to excavate the stone columns at the right place and exactly in the vertical direction. Then, the volume and the weight of an entire stone column were calculated using

16kg/m^3 unit weight, and the column material was weighted and separated. The next step was pulling out the galvanized pipe and after that, compacting the column material. The weighted aggregates were filled in the hole in 5cm layers. The compaction tool, which was made for stone columns, was a special circular tamper with a diameter of 9cm and 2.7kg weight. Each 5cm layer was compacted with 10 blows from 10cm height. This relative density of column material was about 66±5% after this compaction effort. This procedure was repeated until the completion of an OSC.

For the construction of a VESC, the cylindrical encasement mesh should be constructed first. The overlap of the encasement was 2cm and a special polyethylene glue was used to stick this overlap together. Observations demonstrated that the glue operated well, and no opening has happened in the sticking overlap. During the making procedure of VESCs and after digging the hole, the prepared cylindrical encasement was put into the hole; and then filled with the weighted aggregates as 5cm layers and then compacted. The compaction effort was the same as the one used in the construction of OSCs. The steps of the construction of VESCs can be seen in Fig. 4.

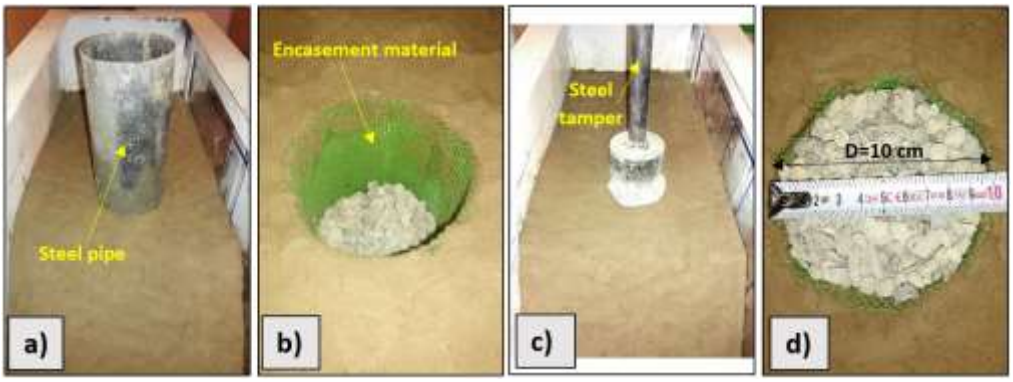

Fig. 4. Construction procedure of a VESC: a**)** penetrating the galvanizes pipe, b) placing the encasement, filling and compacting the aggregates, c) completed column d) checking the diameter of the constructed column.

3. Results and Discussion

Eleven physical tests were carried out on OSCs and VESCs in the current study. The details and bearing capacity results of these tests are reported in Table 2. In this table, Δ is the horizontal spacing between the center of the column and the center of the footing, D is the diameter of the column, L is the length of the stone column and L′ is the length of the encased reinforcement. These parameters are shown in Fig. 1. Some tests were repeated couple of times to increase the confidence in the results.

The loading was applied to the footing using a stress control method. Therefore, the loading value was kept constant until the rate of the changes in the settlement got less than 0.01mm/min. Then, the loading was increased by a constant value, and this procedure was repeated until a failure happened. It should be mentioned that, due to the direct placing of the hydraulic piston on the footing, no tilting was happened in the footing, while in reality the footing can tilt.

Bearing capacity values reported in Table 2 were determined from the pressure-displacement diagrams using the tangent method. Results show that adding any stone column to the slope, had a positive effect on the bearing capacity of the strip footing.

Table 2. Test program and bearing capacities.

Description					Bearing capacity (kPa)
Number of Col.	Col. type	L/D	Δ/D	L′/L	
0	-	-	-	-	99
1	OSC	3	0	-	162
	OSC	4	0	-	203
	OSC	5	0	-	208
	OSC	6	0	-	212
	VESC	4	0	0.25	206
	VESC	4	0	0.5	220
	VESC	4	0	0.75	221
	VESC	4	0	1	226
2	VESC	4	0, 2	1	312
3	VESC	4	0, 2, 4	1	360

Note: In all tests: D=10cm

3.1. Length of Stone Column

The effect of the length of OSCs on the behavior of the footing was investigated for four different lengths. The stone columns with different lengths were placed under the strip footing. The pressure-displacement diagrams of the strip footing which were placed near the slope are depicted in Fig. 5. Results show that a great change in the behavior of footing happened when the length of stone column was changed from 3D to 4D, and the bearing capacity of footing increased about 25%. Also, the settlement of the footing in L=4D state at constant pressure was much less than the settlement of footing in the L=3D state at the same pressure. By increasing the length to L=5D, the improvement in the bearing capacity compared to L=4D state was just about 2%. Moreover, with a further increase in the length of the column to 6D, no significant difference comparing to L=5D state happened, and the bearing capacity increased about 2%. Hence, it can be said that the optimum length of OSCs under the strip footing placed adjacent to a soft clay slope is about four times of their diameter. In rest of the tests, stone columns were constructed with the optimum length of L=40cm. Barksdale and Bachus' [37] have shown that the minimum length of the stone column required for controlling of the bulging failure mode is four times of the diameter. But according to Dash and Bora [35] and Ghazavi and Nazari Afshar [6], the optimum length of stone column to give the maximum performance improvement is five times of its diameter.

The variation of the pressure with column length ratio (L/D) can be seen in Fig. 6 for three constant settlements. This figure shows that a higher pressure is needed when the length of columns is increased to have the same constant settlement. The slope of the curves for all three settlements is sharp between L/D=3 and L/D=4 states, but when the column length ratio further increases to 5 or 6, the slope of the curves becomes mild. It shows that no significant changes have happened in pressures at constant settlements for column length ratios more than four.

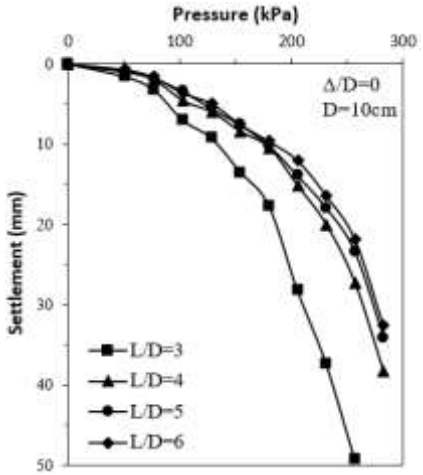

Fig. 5. Test results for different OSC lengths.

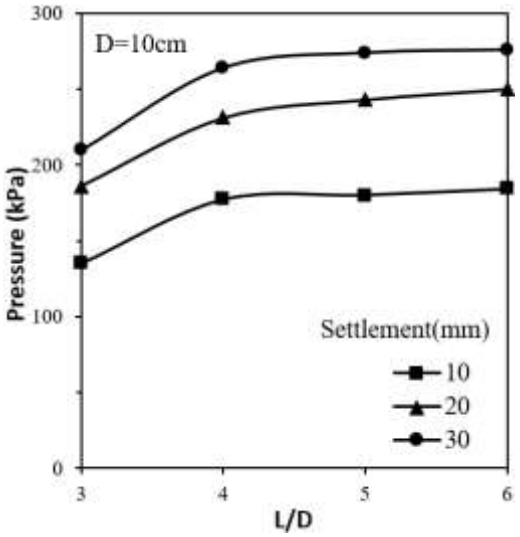

Fig. 6. Variation of pressure with column length ratio.

3.2. length of Vertical Encasement

Effect of length of encasement reinforcement was studied using a series of model tests and the pressure-displacement diagrams of these tests are shown in Fig. 7. Stone columns with all encasement lengths were placed right beneath the footing and the spacing between the center of columns and slope crown was 10cm. When a stone column implements in very soft soil (C_u<15kPa), the column usually fails in bulging due to lack of lateral confinement support that the weak soil can offer [8]. The bulging can typically happen to the upper portion of the stone column [6, 7, 38]. So, different lengths of encasement reinforcement were measured from the top of columns. The bearing capacity observed to increase consistently with increasing the length of the encasement. The largest improve in the bearing capacity happened from 25% encased to 50% encased state. The present findings are in agreement with the observations of Gniel and Bouazza [7], Ghazavi and Nazari Afshar [6] and Dash and Bora [35] that increasing the length of reinforcing encasement, the bearing capacity of stone columns increases.

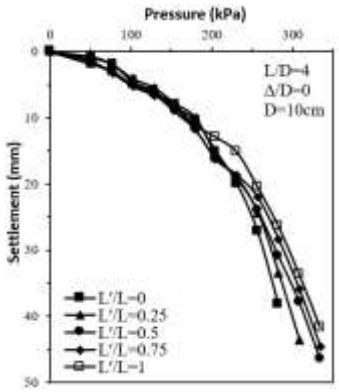

Fig. 7. Test results for different encasement lengths of VESCs.

The variation of pressure with encasement length ratio (L′/L) at constant settlements, is shown in Fig. 8. With the increase in the length of encasement, not a stable trend was seen at settlement equal to 10mm; but for settlements equal to 20mm and 30mm, the pressure was increased gently with the increase of the encasement length.

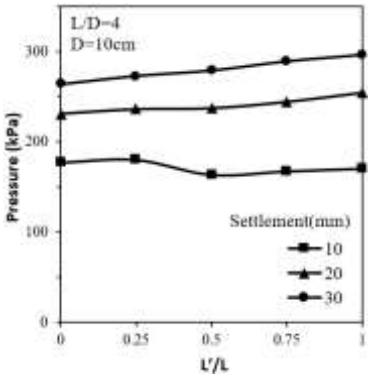

Fig. 8. Variation of pressure with encasement length ratio.

3.3. Group of VESCs

In practice, stone columns are rarely isolated and usually constructed in the group form with a regular pattern. In the current research, an assumed longitudinal slice of the stone column reinforced slope with 30cm width studied. For investigating the influence of group columns, two tests were performed on the groups of two and three VESCs. In both tests, the first column was placed right

beneath the footing and the other columns were placed in the center to center spacing of 20cm (S/D=2) and all columns were fully-encased. the schematic layout and dimensions of the group stone columns are shown in Fig. 9.

The pressure-settlement diagrams for the group of VESCs can be seen in Fig. 10. Results show that with the addition of a greater number of VESCs to the slope, the bearing capacity increased and the settlement in constant pressure decreased severely. For example, the group of three VESCs increased the bearing capacity about 2.64 times compared to no column condition and this shows the positive performance of group stone columns. The pressure diagrams for different numbers of VESCs in the constant displacements are depicted in Fig. 11. Results show that the applied pressure for obtaining each settlement value was increased by increasing the number of VESCs. In other words, with increasing the number of VESCs, a greater pressure is needed to obtain for example a constant settlement equal to 20mm.

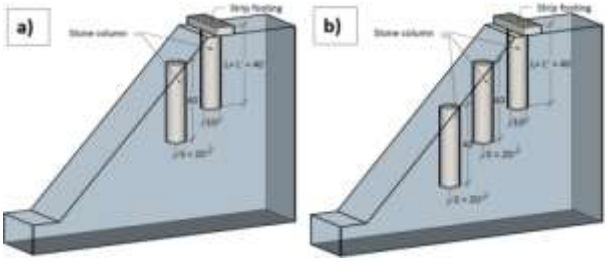

Fig. 9. Schematic layout and dimensions of the group of VESCs (unit: cm): a) two columns b) three columns.

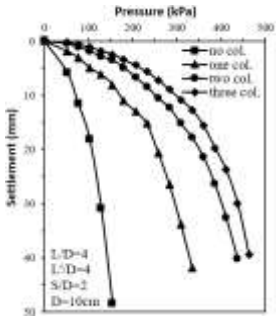

Fig. 10. Test results for different numbers of VESCs.

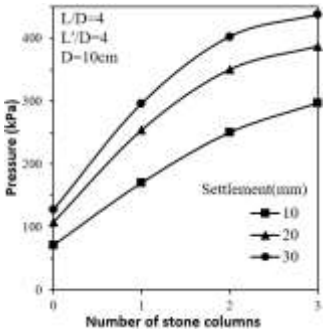

Fig. 11. Variation of stress with number of VESCs.

Also, an efficiency factor (ŋ) for a group of VESCs can be defined as:

$$\eta = \frac{Q_g(u)}{\sum Q_u} \quad (1)$$

In this equation, $Q_g(u)$ represents the bearing capacity of the strip footing near the slope reinforced with a group of VESCs and Q_u represents the bearing capacity of the same footing in the presence of each isolated stone column. The efficiency factor using equation 1, was 83.2% for the group of two VESCs and 72.6% for the group of three VESCs. So, it can be concluded that the group of two VESCs had a better efficiency than the group of three VESCs.

Although there are many parameters influencing on the bearing capacity of a footing near a stone column reinforced slope, but a comparison between the maximum bearing capacity ratio (BCR) of three

experimental articles was gathered in Table 3. The dimensionless factor BCR is defined as the ratio of the bearing capacity of the footing on the stone column reinforced slope to the bearing capacity of the footing on unreinforced slope. In this table S is the spacing between center to center of stone columns, θ is the slope angle, D is the diameter of the stone column, and L is the length of the column.

Table 3. A comparison between the maximum of BCR value.

Reference	Maximum value of BCR	Description
Vekli et al., 2012 [29]	1.72	Ordinary floating stone columns, soft clay soil, S/D=2, D=10cm, L=10cm under the slip surface, θ=33.7°, four columns in the slope with variable lengths
Raee & Hataf, 2018 [31]	1.4	Vertical encased end bearing stone columns, S/D=2, D=6cm, L=66.2cm, one row of three columns
Present study	3.64	Vertical encased floating stone columns, soft clay soil, S/D=2, D=10cm, L=40cm, θ=45°, three columns in the slope

4. Numerical Models

The numerical modeling was performed using the finite element Midas GTS NX (V. 2016) software. The Mohr-Coulomb model was assumed for the soil and the stone column material and the elastic model was assumed for encasement material. The non-linear analysis method was used to analyze the models. Because nonlinear analysis uses iteration methods, the convergence condition can be used to determine whether the solution has converged. The convergence is determined by comparing the displacement, member force or energy change in the previous calculation with the reference values. If all selected conditions are satisfied, the iteration is determined to have converged [39].

Parameters of the numerical modeling are listed in Table 4. In this table the unit weight parameters were determined according to the ASTM D854 test [34]. The internal friction of stone column material was determined by a direct shear test (according to the ASTM D854). The Elastic modulus and the Poisson's ratio of the soil was assumed according to the USACE EM 1110-1-1904 engineer manual [40] because of the limitations of the laboratory equipment. Also the dilation angle of sand was considered by ψ=Ø-30˚ which was suggested in the Midas software manual [39]. Moreover, the internal friction angle and cohesion of the clay was specified by the undrained shear strength tests (according to ASTM D2166-06 [34]).

Triangle meshing was drawn for all the models using the tetra-mesher option in the software. The tetrahedron element can be seen in Fig. 12. The boundary condition in the numerical models was the roller constraints at the front, back, right and left sides and the fixed constraint at the bottom side of the soil. A uniformly distributed load was exerted to the footing. The software automatically considers the self-weight of the soil. The defined load sum was applied in several stages, as an increment, cumulatively. Obviously, more stages of loading make the analysis process longer. Also, each contact between three materials (footing, clay soil, and stone column) was defined using the

general contact option in the Midas software. General contact considers the impact and the impact friction between two objects in the analysis. In Fig. 12 a sample of 3D numerical modeling and the mesh arrange for the group of three stone columns are demonstrated.

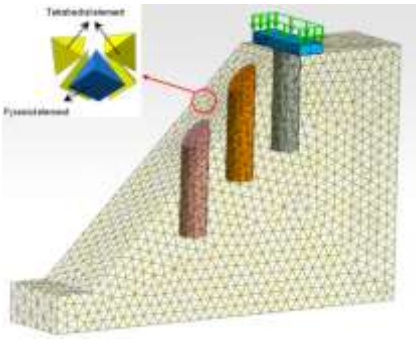

Fig. 12. numerical modeling of a group of three stone columns.

Table 4. Parameters of numerical modeling.

Parameter	Value			
	Clay	Stone column material	Footing material	Encasement
Unit weight (kN/m^3)	20	16	78	2
Cohesion (kPa)	8	0.1	-	-
Internal friction angle (Ø˚)	0	45	-	-
Poisson's ratio	0.45	0.3	0.3	0.3
Modulus of elasticity (kPa)	2000	60000	2E8	16000
Dilation angle (ψ˚)	0	15	-	-

4.1. Verification of Numerical Results

In order to verify the numerical results, two experimental tests which were accomplished by Debnath and Dey [41] were modeled in the Midas software and the results were compared. The first modeled test was the clay bed without any stone column and the second was the clay bed reinforced with twelve OSCs in a triangular pattern. The diameter of stone column was 5cm and the length of them was 30cm in both tests. A circular steel plate with a diameter of 20cm was placed on the three middle columns and the loading was exerted to this plate. The meshing and the arrangement of stone columns in this model can be seen in Fig. 13. The whole dimensions and material parameters in the numerical modeling were assumed equal to the dimensions and parameters which were assumed by Debnath and Dey [41]. The comparison between the results of numerical and physical modeling is shown in Fig. 14. Diagrams showed a relatively good agreement between the results. In this figure, S is footing settlement and D is stone column diameter which was equal to 5cm.

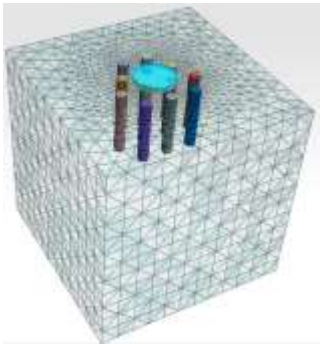

Fig. 13. Meshing and geometry of finite element model.

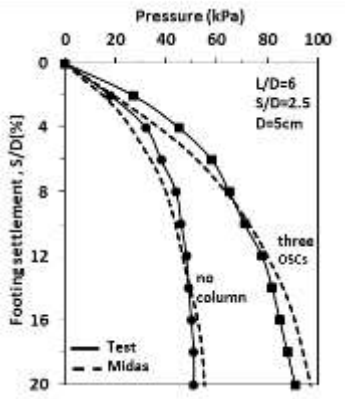

Fig. 14. Verification of numerical results with tests carried out by Debnath and Dey [41].

4.2. Stress Distribution and Deformations

In this part of the article, a series of results from numerical modeling will be presented for a better illustration of the stone column reinforced slope. A sample of the total displacement of the slope with the presence of one OSC can be seen in Fig. 15. This figure shows the displacement after loading in both experimental and numerical modeling. Both observations showed that the footing was penetrated into the soil and the top part of the slope (near the crown) was swelled. The swelling location was almost the same in the both numerical and laboratory results. Stress distributions for the group of three OSCs and three VESCs are shown in Fig. 16. One longitudinal section and one cross-section from the center of the footing was drawn in this figure for a better visibility of stress distributions. Both parts of this figure showed that the stone columns which were placed under the footing carried more stress than the others, because of the different operation mechanism they had. Comparing both parts of this figure also showed that, the stress was spread around the OSCs but with vertical encasing the stone columns, the stress was concentrated in the stone column. Therefore, the encasement caused an integrated operation of the stone column. Furthermore, the third column carried more stress comparing to the second stone column in both OSC and VESC states.

4.3. Factor of Safety of Slope Stability

The factor of safety of the slopes is a very important issue in geotechnical engineering and many of researchers always have concerns about that. One method of calculation of the safety factor in finite element programs is reducing the shear strength parameters (c and tanφ) of the soil, until the slope failure occurs. This method is considered in the Midas software as strength reduction method (SRM) in the solution type menu. In this method, the vertical encasement of the stone columns cannot be modeled and have no influence on the factor of safety results. Therefore, the results are presented just for OSCs and the effect of stone column location and group of stone columns on the safety factors was studied. The approximate critical slip surface of the slope can be observed from the shear strain contour [42]. So, the slip surfaces of the slope were obtained from the shear strain contours in the software. The factor of safety of the unreinforced slope under no loading was equal to 2.607. For a better understanding of the results, a parameter called improvement factor (I_f) was defined as below:

$$I_f = \frac{FS_{reinforced}}{FS_{unreinforced}} \quad (2)$$

Where $FS_{reinforced}$ is the safety factor of the slope reinforced with stone column, and $FS_{unreinforced}$ is the safety factor of the unreinforced slope in the same conditions.

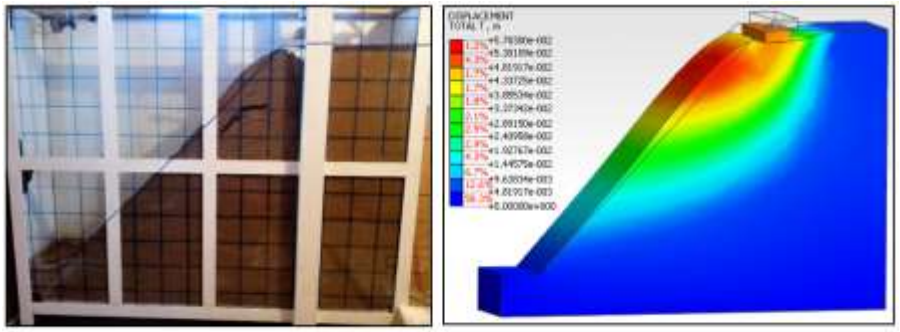

a) b)

Fig. 15. Total displacements for one OSC a) physical modeling b) numerical modeling.

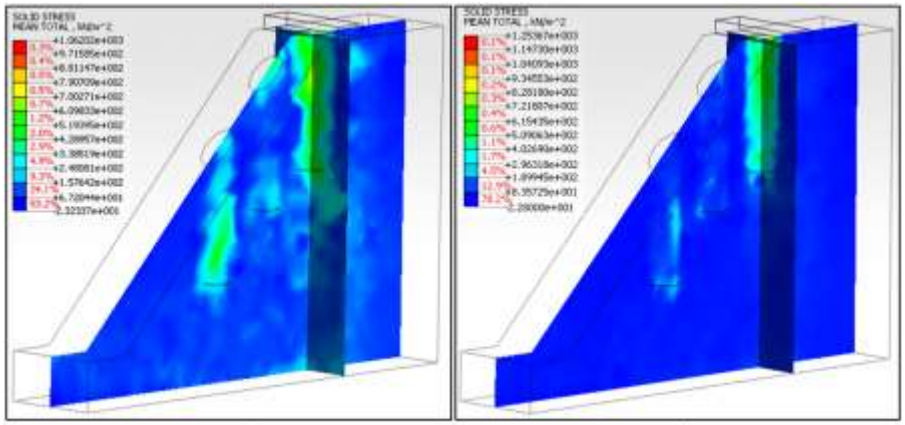

a) b)

Fig. 16. Total stress in two sections from the center of footing a) Three OSCs b) Three VESCs.

4.3.1. optimum Location of Stone Column

One of the most important parameters in the slope stabilization with a column-like element is the optimum location of this element. The X_f and L_x parameters were defined in Fig. 17 for a better illustration of the location of stone column in the slope. The FS values obtained from the Midas software are reported in Table 5. In the analyses of this part, a stone column was added to the different locations of the slope and the footing was loaded with different uniform loadings (q). Then the FS values were calculated for different conditions. It can be seen that with increasing the loading value, the FS values were decreased severely.

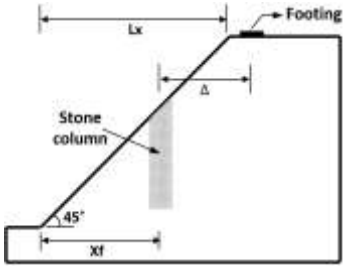

Fig. 17. parameters definition for optimum location of stone column.

The critical slip surfaces of slope for different locations of stone columns under the loading state q=150kPa are shown in Fig. 18. Results show that when there was no stone column, the critical slip surface was general and continues to the toe of the slope. But when a stone column was added to the slope, the slip surface was local and almost continued to the middle part of the slope. The

variations of improvement factor (I_f) with the location of the stone column are depicted in Fig. 19. The diagrams are once shown according to Δ/D values and the other time are shown based on X_f/L_x values. The maximum influences of the stone column on the improvement of FS were happened in the state with no loading on the footing (q=0). In this state, adding a stone column in Δ/D=4 position was led to a 68% increase in the FS value. With loading of the footing (q≠0), the influences of the stone column on the FS values were reduced severely. The Δ/D=1 state showed the lowest values of I_f and the Δ/D=4 state showed the highest values of I_f. It means that the optimum location of the stone column for improving the FS is X_f/L_x=0.65 and with increasing the X_f more than this value, the I_f is reduced. A summary of the optimum location of stone columns and piles is presented in Table 6. Most of the researchers reported that the optimum location of stone columns or piles for improving the FS is the middle or upper middle of the slope.

Table 5. Factor of safety for different locations of stone column and different loadings.

Description		Factor of safety (FS)				
		q=0	q=50kPa	q=100kPa	q=150kPa	q=200kPa
Δ/D=0	-	4.325	2.131	1.291	1.006	0.842
Δ/D=1	Xf/Lx=1	4.281	2.002	1.166	0.875	0.732
Δ/D=2	Xf/Lx=0.88	4.338	2.124	1.297	0.994	0.816
Δ/D=3	Xf/Lx=0.76	4.278	2.128	1.320	1.009	0.838
Δ/D=4	Xf/Lx=0.65	4.388	2.209	1.342	1.025	0.853
Δ/D=5	Xf/Lx=0.53	4.313	2.184	1.322	1.020	0.858
Δ/D=6	Xf/Lx=0.41	4.306	2.208	1.331	1.016	0.848

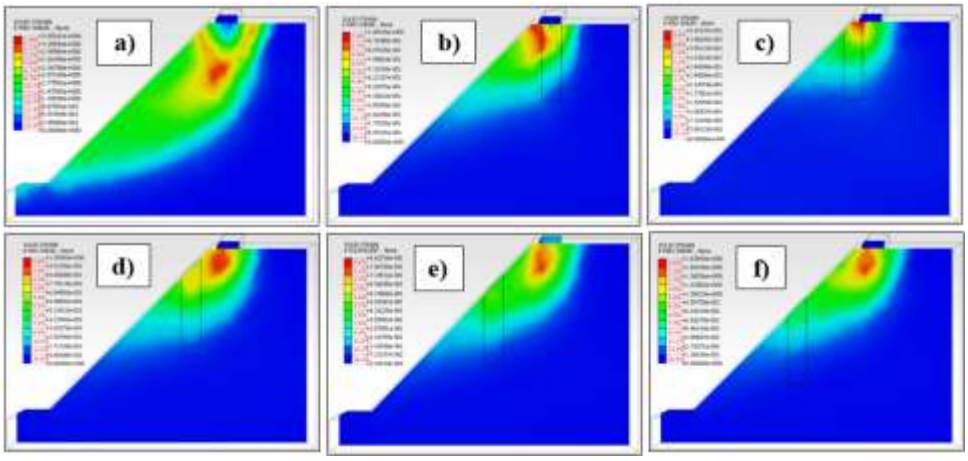

Fig. 18. Critical slip surfaces a) no stone column b) Δ /D=0 c) Δ /D= 1 d) Δ /D= 2 e) Δ /D= 3 f) Δ /D= 4.

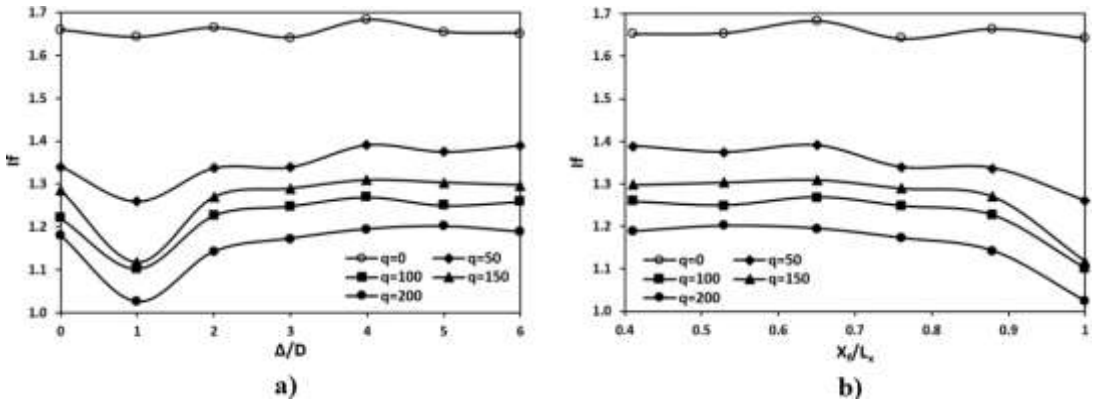

Fig. 19. Variation of I_f with stone column location (Loading unit: kPa) a) according to Δ /D b) according to X_f/L_x.

Table 6. Comparison of the optimum location of vertical elements added to the slope.

Reference	Description	Optimum location (X_f/L_x)
Nasiri and Hajiazizi [33]	Numerical, slope stabilized with stone column, Flac 3D software, sandy soil	0.5
Paresh and Vasanwala [43]	Numerical, slope stabilized with one row of stone column, Plaxis 2D software, clayey soil	0.75
Ghazavi and Shahmandi [28]	Analytical, slope stabilized with one row of stone column, limit equilibrium method, soft clayey soil	1
Li et al. [22]	Numerical, slope stabilized with one row of pile, Flac 2D software, clayey soil	0.51
Sun et al. [42]	Numerical, slope stabilized with one row of micropile, Flac 3D software, clayey soil	0.7
Wei and Cheng [44]	Numerical, slope stabilized with one row of pile, Flac 3D software, clayey soil	0.54
Present study	Numerical, slope stabilized with stone column, Midas software, soft clayey soil	0.65

4.3.2. Group of OSCs

In this part of the article, the effect of number of OSCs on the safety factor of the slope was investigated. The arrangement and the dimensions of the stone column in this part were the same as part 3-3 of the current article. The FS results for different number of OSCs and different loading values are provided in Table 7. Results show that by increasing the number of stone columns, the safety factor was increased in all states of the loading. Although adding a single stone column to the slope had the most influence on the FS. Also, with increasing the amount of loading the safety factor value was decreased.

The variation of I_f with the number of stone columns is depicted in Fig. 20. The greatest influence on the FS is related to the slope under no loading. Adding one OSC in this

condition was led to a 66% increase and adding four OSCs was led to an 87% increase in the FS value. Although, with applying the load on the footing the FS values were decreased extremely comparing to no loading condition. The highest rate of changes in I_f between all amounts of loadings, was between no column and one column states.

Table 7 Factor of safety for different number of stone columns and different loadings

Description	Factor of safety (FS)				
	q=0	q=50kPa	q=100kPa	q=150kPa	q=200kPa
No column	2.607	1.589	1.058	0.783	0.714
One column	4.325	2.131	1.291	1.006	0.842
Two columns	4.413	2.150	1.353	1.022	0.884
Three columns	4.700	2.228	1.369	1.047	0.895
Four columns	4.888	2.263	1.384	1.059	0.909

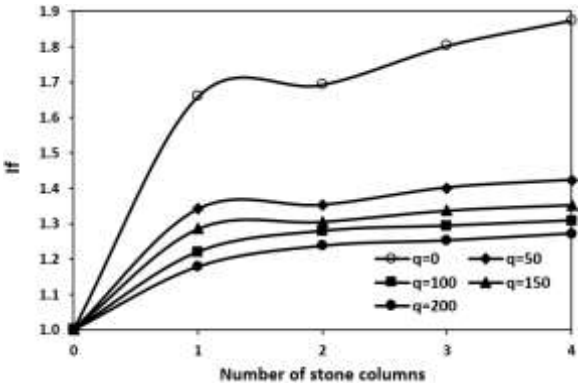

Fig. 20. Variation of I_f with number of OSCs.

5. Conclusions

In this investigation, some model tests on a strip footing adjacent to a stone column reinforced clayey slope were carried out. In total, 11 tests were carried out and different parameters such as the length of stone column and the length of vertical encasement were studied. Also, the influence of the group of VESCs on the behavior of strip footing was examined. Moreover, some finite element analyses were performed and the factor of safety of the slope was studied. The following major conclusions may be obtained from numerical and experimental results:

1- Reinforcing the slope with the stone column in all tests causes an increase in the bearing capacity of the strip footing and a decrease in the settlement. Vertical incasing of the stone columns leads to a further improvement in the behavior of the footing.

2- The optimum length of an ordinary stone column (OSC) which is placed beneath the strip footing is 4 times their diameter. Further increasing the length ratio (L/D) to values of 5 and 6, leads to just about 2% and 4% improvement in the bearing capacity of footing compared to L/D=4 state.

3- With increasing the length of encasement from non-encased to fully encased state, the bearing capacity of footing increases consistently. The maximum variation in the bearing capacity of the strip footing happens when the encasement length changes from 25% to 50% of the column length. In total, the influence of encasement length on the behavior of the footing is gentler than the influence of the other

parameters such as length of the stone column.

4- Investigating the efficiency factor for the group of vertical encased stone columns (VESCs) shows that, the group of two columns has a better efficiency compared to the group of three columns.

5- The best location of an OSC in the slope for achieving the highest safety factor is in the upper middle of the slope (X_f/L_x=0.65).

6- With increasing the number of OSCs added to slope, the factor of safety increases. Also, the results show that in the unreinforced slope, the critical slip surface is general and continues to the toe of the slope. But in the stone column reinforced slope, the slip surface is local and almost continues to the middle part of the slope.

REFERENCES

[1] A. Ambily, S.R. Gandhi, (2007). Behavior of stone columns based on experimental and FEM analysis, Journal of geotechnical and geoenvironmental engineering, 133(4) 405-415. DOI: 10.1061/(ASCE)1090-0241(2007)133:4(405)

[2] J. Shahu, Y. Reddy, (2011). Clayey soil reinforced with stone column group: model tests and analyses, Journal of Geotechnical and Geoenvironmental Engineering, 137(12) 1265-1274. DOI: 10.1061/(ASCE)GT.1943-5606.0000552

[3] G. Kumar, M. Samanta, (2020). Experimental evaluation of stress concentration ratio of soft soil reinforced with stone column, Innovative Infrastructure Solutions, 5(1) 18. DOI: 10.1007/s41062-020-0264-6

[4] J. Nazariafshar, N. Mehrannia, F. Kalantary, N. Ganjian, (2019). Bearing capacity of group of stone columns with granular blankets, International Journal of Civil Engineering, 17(2) 253-263. DOI: 10.1007/s40999-017-0271-y

[5] J.M.O. Hughes, N.J. Withers, (1974). Reinforcing of soft cohesive soils with stone columns, International Journal of Rock Mechanics and Mining Sciences & Geomechanics, 11(11) A234.

[6] M. Ghazavi, J.N. Afshar, (2013). Bearing capacity of geosynthetic encased stone columns, Geotextiles and Geomembranes, 38 26-36. DOI: 10.1016/j.geotexmem.2013.04.003

[7] J. Gniel, A. Bouazza, (2009). Improvement of soft soils using geogrid encased stone columns, Geotextiles and Geomembranes, 27(3) 167-175. DOI: 10.1016/j.geotexmem.2008.11.001

[8] C. Cengiz, E. Güler, (2018). Seismic behavior of geosynthetic encased columns and ordinary stone columns, Geotextiles and Geomembranes, 46(1) 40-51. DOI: 10.1016/j.geotexmem.2017.10.001

[9] M. Miranda, A. Da Costa, J. Castro, C. Sagaseta, (2017). Influence of geotextile encasement on the behaviour of stone columns: Laboratory study, Geotextiles and Geomembranes, 45(1) 14-22. DOI: 10.1016/j.geotexmem.2016.08.004

[10] S. Nayak, M.P. Vibhoosha, A. Bhasi, (2019). Effect of Column Configuration on the Performance of Encased Stone Columns with Basal Geogrid Installed in Lithomargic Clay, International Journal of Geosynthetics and Ground Engineering, 5(4) 29. DOI: 10.1007/s40891-019-0181-y

[11] C. Yoo, Q. Abbas, (2020). Laboratory investigation of the behavior of a geosynthetic encased stone column in sand under cyclic loading, Geotextiles and Geomembranes. DOI: 10.1016/j.geotexmem.2020.02.002

[12] Y.-S. Hong, C.-S. Wu, C.-M. Kou, C.-H. Chang, (2017). A numerical analysis of a fully penetrated encased granular column, Geotextiles and Geomembranes, 45(5) 391-405. DOI: 10.1016/j.geotexmem.2017.05.002

[13] A.J. Choobbasti, H. Pichka, (2014). Improvement of soft clay using installation of geosynthetic-encased stone columns: numerical study, Arabian Journal of

Geosciences, 7(2) 597-607. DOI: 10.1007/s12517-012-0735-y

[14] J. Castro, (2017). Groups of encased stone columns: Influence of column length and arrangement, Geotextiles and Geomembranes, 45(2) 68-80. DOI: 10.1016/j.geotexmem.2016.12.001

[15] A. Ehsaniyamchi, M. Ghazavi, (2019). Short-term and long-term behavior of geosynthetic-reinforced stone columns, Soils and Foundations, 59(5) 1579-1590. DOI: 10.1016/j.sandf.2019.07.007

[16] M.A. Nav, R. Rahnavard, A. Noorzad, R. Napolitano, (2020) Numerical evaluation of the behavior of ordinary and reinforced stone columns, Structures, 25 481-490. DOI: 10.1016/j.istruc.2020.03.021

[17] M.S. Keskin, M. Laman, (2014). Experimental and numerical studies of strip footings on geogrid-reinforced sand slope, Arabian Journal for Science and Engineering, 39(3) 1607-1619. DOI: 10.1007/s13369-013-0795-7

[18] M.A. El Sawwaf, (2007). Behavior of strip footing on geogrid-reinforced sand over a soft clay slope, Geotextiles and Geomembranes, 25(1) 50-60. DOI: 10.1016/j.geotexmem.2006.06.001

[19] A. Sommers, B. Viswanadham, (2009). Centrifuge model tests on the behavior of strip footing on geotextile-reinforced slopes, Geotextiles and Geomembranes, 27(6) 497-505. DOI: 10.1016/j.geotexmem.2009.05.002

[20] S. Naeini, B.K. Rabe, E. Mahmoodi, (2012). Bearing capacity and settlement of strip footing on geosynthetic reinforced clayey slopes, Journal of Central South University, 19(4) 1116-1124. DOI: 10.1007/s11771-012-1117-z

[21] N. Hataf, A. Fatolahzadeh, (2019). An experimental and numerical study on the bearing capacity of circular and ring footings on rehabilitated sand slopes with geogrid, Journal of Rehabilitation in Civil Engineering, 7(1) 174-185. DOI: 10.22075/JRCE.2018.11576.1193

[22] X. Li, S. He, Y. Luo, Y. Wu, (2011). Numerical studies of the position of piles in slope stabilization, Geomechanics and Geoengineering, 6(3) 209-215. DOI: 10.1080/17486025.2011.578668

[23] M. Ashour, H. Ardalan, (2012). Analysis of pile stabilized slopes based on soil–pile interaction, Computers and Geotechnics, 39 85-97. DOI: 10.1016/j.compgeo.2011.09.001

[24] M. Esmaeili, M. Gharouni Nik, F. Khayyer, (2013). Static and Dynamic Analyses of Micropiles to Reinforce the High Railway Embankments on Loose Beds, Journal of Rehabilitation in Civil Engineering, 1(2) 80-89. DOI: 10.22075/JRCE.2013.11

[25] Z. Zhang, J. Han, G. Ye, (2014). Numerical investigation on factors for deep-seated slope stability of stone column-supported embankments over soft clay, Engineering Geology, 168 104-113. DOI: 10.1016/j.enggeo.2013.11.004

[26] J.-F. Chen, L.-Y. Li, J.-F. Xue, S.-Z. Feng, (2015). Failure mechanism of geosynthetic-encased stone columns in soft soils under embankment, Geotextiles and Geomembranes, 43(5) 424-431. DOI: 10.1016/j.geotexmem.2015.04.016

[27] G. Zheng, X. Yu, H. Zhou, S. Wang, J. Zhao, X. He, X. Yang, (2020). Stability analysis of stone column-supported and geosynthetic-reinforced embankments on soft ground, Geotextiles and Geomembranes. DOI: 10.1016/j.geotexmem.2019.12.006

[28] M. Ghazavi, A. Shahmandi, (2008). Analytical Static Stability Analysis of Slopes Reinforced by Stone, The 12th International Conference of International Association for Computer Methods and Advances in Geomechanics (IACMAG), India, 3530-3537.

[29] M. Vekli, M. Aytekin, S.B. Ikizler, Ü. Çalik, (2012). Experimental and numerical investigation of slope stabilization by stone columns, Natural hazards, 64(1) 797-820. DOI: 10.1007/s11069-012-0272-8

[30] M. Hajiazizi, E. Nemati, M. Nasiri, M. Bavali, M. Sharifipur, (2012). Optimal Location of Stone Column in Stabilization of Sand Slope: An Experimental and 3D

Numerical Investigation, Scientia Iranica. DOI: 10.24200/SCI.2018.20331

[31] E. Raee, N. Hataf, K. Barkhordari, A. Ghahramani, (2018). The Effect of Rigidity of Reinforced Stone Columns on Bearing Capacity of Strip Footings on the Stabilized Slopes, International Journal of Civil Engineering, 1-13. DOI: 10.1007/s40999-018-0291-2

[32] E. Naderi, A. Asakereh, M. Dehghani, (2018). Bearing Capacity of Strip Footing on Clay Slope Reinforced with Stone Columns, Arabian Journal for Science and Engineering, 43(10) 5559-5572. DOI: 10.1007/s13369-018-3231-1

[33] M. Nasiri, M. Hajiazizi, (2019). An experimental and numerical investigation of reinforced slope using geotextile encased stone column, International Journal of Geotechnical Engineering, 1-10. DOI: 10.1080/19386362.2019.1651029

[34] A.S.f.T.a. Materials, ASTM, (1984). American Society for Testing.

[35] S.K. Dash, M.C. Bora, (2013). Influence of geosynthetic encasement on the performance of stone columns floating in soft clay, Canadian Geotechnical Journal, 50(7) 754-765. DOI: 10.1139/cgj-2012-0437

[36] D.M. Wood, W. Hu, D.F.T. Nash, (2000). Group effects in stone column foundations: model tests, Géotechnique, 50(6) 689-698. DOI: 10.1680/geot.2000.50.6.689

[37] R. Barksdale, R. Bachus, (1983). Design and Construction of Stone Columns Volume II, Appendixes, Federal Highway Administration Washington, DC, USA.

[38] M. Hasan, N. Samadhiya, (2017). Performance of geosynthetic-reinforced granular piles in soft clays: Model tests and numerical analysis, Computers and Geotechnics, 87 178-187. DOI: 10.1016/j.compgeo.2017.02.016

[39] MIDAS/GTS NX. manual, (2016). Modeling, Integrated Design & Analysis Software. A geotechnical and tunnel analysis system.

[40] USACE, (1990). Settlement Analysis, Engineer Manual EM 1110-1-1904.

[41] P. Debnath, A.K. Dey, (2017). Bearing capacity of geogrid reinforced sand over encased stone columns in soft clay, Geotextiles and Geomembranes, 45(6) 653-664. DOI: 10.1016/j.geotexmem.2017.08.006

[42] S.-W. Sun, W. Wang, F. Zhao, (2014). Three-dimensional stability analysis of a homogeneous slope reinforced with micropiles, Mathematical Problems in Engineering, 2014 1-11. DOI: 10.1155/2014/864017

[43] P. Paresh, S. Vasanwala, (2012). Numerical analysis of slope reinforced with stone column, Int. journal of civil, structural, environmental and infrastructure engineering research and development, 2(2) 7.

[44] W. Wei, Y. Cheng, (2009). Strength reduction analysis for slope reinforced with one row of piles, Computers and Geotechnics, 36(7) 1176-1185. DOI: 10.1016/j.compgeo.2009.05.004